

N-Terminally Truncated Amyloid- $\beta_{(11-40/42)}$ Co-Fibrillises with its Full-Length Counterpart, Implications for Alzheimer's Disease.

Joseph D. Barritt^[b], Nadine D. Younan^[c] and John H. Viles^{*[a]}

Abstract: Amyloid- β peptide ($A\beta$) isoforms of different lengths and aggregation propensities coexist *in vivo*. These different isoforms are able to nucleate or frustrate the assembly of each other. N-terminal truncated $A\beta_{(11-40)}$ and $A\beta_{(11-42)}$ make up one fifth of plaque load yet nothing is known about their interaction with full-length $A\beta_{(1-40/42)}$. Here we show that in contrast to C-terminal truncated isoforms which do not co-fibrillise, deletions of ten residues from the N-terminus of $A\beta$ have little impact on its ability to co-fibrillise with the full-length counterpart. As a consequence N-terminal truncated $A\beta$ will accelerate fibre formation and co-assemble into short rod-shaped fibres with its full-length $A\beta$ counterpart. This has implications for the assembly kinetics, morphology and toxicity of all $A\beta$ isoforms.

Misfolding and self-assembly of an endogenous peptide, amyloid- β ($A\beta$), into toxic oligomers and amyloid fibres is central to the amyloid cascade in Alzheimer's Disease (AD) [1]. The 40 or 42 amino acids long peptide, $A\beta_{(1-40/42)}$, is released as a cleavage product of the amyloid precursor protein (APP), by the action of the β - and γ -secretase complex. However both the β - and γ -secretases have variable site specificity for APP and produce different lengths of $A\beta$ [2]. The main N-truncated form of $A\beta$ is generated by secondary β -secretase activity (β') which produces $A\beta_{(11-40/42)}$ [3], although other N-truncated and extended forms of $A\beta$ are also formed [4]. $A\beta_{(11-40/42)}$ is at least as abundant as $A\beta_{(1-42)}$ in the cerebrospinal fluid (CSF) [5] and makes up one-fifth of plaque load [6]. Intriguingly, $A\beta_{(11-40/42)}$ and the N-terminal pyroglutamate form are concentrated at the core of plaques in AD brains [7]. Furthermore, some familial forms of AD are noted for increasing the level of $A\beta_{(1-42)}$ but also elevate levels of $A\beta_{(11-42)}$ by as much as 33-42% [8]. There is much interest in the interaction of $A\beta_{(1-40)}$ with $A\beta_{(1-42)}$, that are both present in plaques, as changes in the ratio of 42/40 are linked with inherited AD [9]. It is clear that one $A\beta$ isoform influences the fibre formation kinetics of the other [10].

Despite $A\beta_{(11-40/42)}$ being a major component of plaques and CSF (20 % of plaque load) [5-6], there has been little biophysical characterisation of N-terminally truncated $A\beta$. We have recently shown that $A\beta_{(11-40/42)}$ binds Cu^{2+} with an extremely tight femtomolar affinity and forms amyloid fibres much more rapidly than $A\beta_{(1-40)}$ [11]. Here we aim to probe the impact $A\beta_{(11-40/42)}$ has on the amyloid assembly of full-length $A\beta$ isoforms. This study provides insight into the role of the first ten residues in the protofibril assembly pathway and the impact on the kinetics of assembly and fibre stability; both in isolation and in

physiologically relevant mixtures.

In marked contrast to full-length $A\beta_{(1-40)}$ and $A\beta_{(1-42)}$, quiescently grown fibres of $A\beta_{(11-40)}$ and $A\beta_{(11-42)}$ readily fragmented with mild agitation, generating short amyloid rods, with a mean length of 150 nm, see supplemental figure S1 and S2. Although residues 1-10 are not thought to form hydrogen-bonded strands in $A\beta_{(1-40)}$ or $A\beta_{(1-42)}$ fibres [12], it is clear they contribute to stability of the fibres and resistance to mechanical shear forces. A similar tendency to fragment has been reported for another N-terminal truncated form of $A\beta$, residues 4-40 [4b]. We also addressed the possibility that the loss of the ten N-terminal residues may modulate formation of prefibrillar assemblies. TEM micrographs show a snap-shot of the prefibrillar structural morphologies present at given times during $A\beta_{(11-40)}$ and $A\beta_{(11-42)}$ assembly, supplemental figure S3, S4 and S5. Very similar circular oligomeric structural morphologies, between 5-40 nm in diameter, and curvy-linear protofibrillar structures were observed, in the early stages of assembly, across all isoforms irrespective of the N-terminal truncation. In contrast to current understanding [13], our TEM studies show the first ten residues of $A\beta$ are not a requirement for the formation of oligomers and curvy protofibrillar assemblies.

Although $A\beta_{(11-40/42)}$ is a major component of plaques, nothing is known about how it might influence $A\beta_{(1-40/42)}$ fibre formation. ThT fluorescence was used to monitor fibre formation of $A\beta_{(1-40)}$ and $A\beta_{(11-40)}$ mixtures, under the influence of mild agitation. Both isoforms produce time-dependent ThT fluorescence signals with a sigmoidal curve associated with a slow lag-phase (nucleation) followed by rapid fibre elongation as $A\beta$ monomer is recruited to the growing ends of fibres, before the maximal signal plateaus at equilibrium, figure 1A. $A\beta_{(11-40)}$ lag-times (19 ± 1 hrs) are markedly shorter than $A\beta_{(1-40)}$ (99 ± 3 hrs) under identical conditions. Next the ThT signal was monitored for equimolar mixtures of $A\beta_{(11-40)}$ and $A\beta_{(1-40)}$, figure 1A. The ThT traces have a lag-phase of 61 ± 1 hours; an intermediate time between $A\beta_{(11-40)}$ and $A\beta_{(1-40)}$. Fibre formation of $A\beta_{(1-40)}$ is accelerated by the presence of $A\beta_{(11-40)}$. Indeed the mixed isoforms have intermediate formation kinetics which linearly correlate with the ratio of $A\beta_{(11-40)}$ and $A\beta_{(1-40)}$, supplemental figure S6. The combined rate constants for nucleation and elongation are a weighted average of the rate constants for the $A\beta$ isoforms in isolation, supplemental figure S6. Any mixed assemblies that form, do not slow fibre formation of $A\beta_{(1-40)}$ suggesting they are not off-pathway and form part of the final fibre. This behaviour with the absence of a biphasic curve raises the possibility that $A\beta_{(11-40)}$ and $A\beta_{(1-40)}$ might co-fibrillise. This is supported by the markedly different fibre formation kinetics observed for mixtures of $A\beta_{(11-40)}$ with $A\beta_{(1-42)}$, figure 1b and supplemental figure S7. Rather than accelerating $A\beta_{(1-42)}$ fibre formation, as was observed for $A\beta_{(1-40)}$, the $A\beta_{(11-40)}$ with $A\beta_{(1-42)}$ mixture has frustrated fibre formation kinetics. In this case the equimolar mixture has a longer lag-phase than both $A\beta_{(11-40)}$ and $A\beta_{(1-42)}$ individually; 62 ± 3 hours for the binary mixture, compared to lag-times of 6.6 ± 0.3 hours and 37 ± 2 hours respectively. Suggesting for this $A\beta$ isoform combination initial co-aggregated oligomers are off-pathway to forming individual fibres and so slow fibre assembly. Furthermore this

- [a] Dr J.H. Viles (Corresponding Author)
Department Chemistry and Biochemistry, Queen Mary, University of London, Mile End Road, London E1 4NS, UK
j.viles@qmul.ac.uk
- [b] Dr J.D. Barritt, Department Chemistry and Biochemistry, Queen Mary, University of London, Mile End Road, London E1 4NS, UK
joseph.barritt@imperial.ac.uk
- [c] Dr N.D. Younan, Department Chemistry and Biochemistry, Queen Mary, University of London, Mile End Road, London E1 4NS, UK
n.d.younan@qmul.ac.uk

Supporting information for this article is given via a link at the end of the document

combination of isoforms produces biphasic kinetic behaviour, which is consistent with independent fibre formation, see supplemental figure S7 in particular. Biphasic kinetics has also recently been reported for $A\beta_{(1-40)}$ with $A\beta_{(1-42)}$ mixtures [10d].

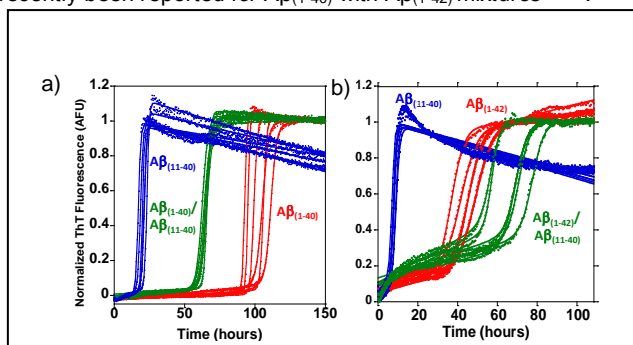


Figure 1. Fibrillation of $A\beta_{(11-40)}$ with full-length $A\beta$. Fiber formation monitored by ThT fluorescence. Equimolar mixture of $A\beta_{(11-40)}$ and $A\beta_{(1-40)}$ (green) compared with $A\beta_{(11-40)}$ (blue) and $A\beta_{(1-40)}$ (red) kinetic traces (a). Equimolar mixture of $A\beta_{(11-40)}$ and $A\beta_{(1-42)}$ (green) compared with $A\beta_{(11-40)}$ (blue) and $A\beta_{(1-42)}$ (red) kinetic traces (b), at pH 7.4, total $A\beta$ 10 μM , $n = 6$ traces,

The strongest support for a high proportion of co-fibrillation for $A\beta_{(11-40)/(1-40)}$ but not $A\beta_{(11-40)/(1-42)}$ comes from TEM data. In mixtures of $A\beta_{(11-40)/(1-40)}$, only short rod-like fibres are observed, similar in length to $A\beta_{(11-40)}$ in isolation, figure 2a. If $A\beta_{(11-40)}$ and $A\beta_{(1-40)}$ form fibres independently one would expect very long fibres to also be present, as is observed for $A\beta_{(1-40)}$ in isolation. Quantification of fibre length distribution, (figure 2a) indicates only very short fibres (<400 nm) are consistently present. Incorporation of $A\beta_{(11-40)}$ into $A\beta_{(1-40)}$ fibres imparts these fibres with a similar susceptibility to shear forces as isolated $A\beta_{(11-40)}$. This behaviour is in marked contrast to the binary mixture of $A\beta_{(11-40)/(1-42)}$ this mixture does not co-fibrillise and these fibres form independently. For this mixture, there is an equal proportion of long fibres, very similar in length distribution to $A\beta_{(1-42)}$, together with very short fibre-rods very similar in length distribution to $A\beta_{(11-40)}$, shown in figure 2b.

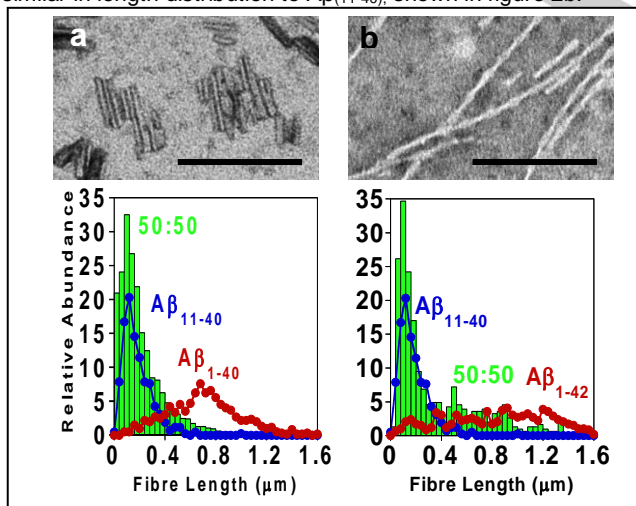


Figure 2: Fibre length distribution for $A\beta$ isoforms in isolation and as mixtures. A binary mixture of $A\beta_{(11-40)}$ with $A\beta_{(1-40)}$, exclusively short fibre rods are present < 400 nm, indicating cofibrillation (a). $A\beta_{(11-40)}$ with $A\beta_{(1-42)}$ binary mixture; combination of short and long fibres are present, indicating the isoforms form fibres separately (b). TEM scale bar 200 nm. Typically >2000 fibre lengths were measured per condition.

Similarly fibre length distributions have been quantified for $A\beta_{(11-42)+(1-40)}$ and $A\beta_{(11-42)+(1-42)}$ binary mixtures, see supplemental figure S8. $A\beta$ isoforms with the same C-termini co-fibrillise producing only short amyloid rods. In contrast, $A\beta_{(11-42)+(1-40)}$ produce fibres independently and exhibit both long fibres and short rods.

To further support the assertion $A\beta_{(11-40)}$ and $A\beta_{(1-40)}$ fibres co-assemble we used $^1\text{H-NMR}$ to monitor fibre growth. Spectra of $A\beta_{(11-40)}$ and $A\beta_{(1-40)}$ in D_2O at pH 7.4 reveal well resolved and characteristic δH resonances for His13 and His14, these peaks are shifted downfield for the $A\beta_{(11-40)}$ peptide at pH 7.4, as shown in figure 3A. Tyr10 and His6 side chain resonances were assigned for $A\beta_{(1-40)}$ but are absent in the $A\beta_{(11-40)}$ spectra. 1D $^1\text{H-NMR}$ spectra of an equimolar mixture of both peptides were acquired over several hours with mild agitation generated by cycles of sample spinning in the NMR tube between spectra acquisitions. The increase in line-width and consequent complete loss of signal for fibre assemblies (which are megadaltons in size) can be plotted over time to monitor the rate of loss of $A\beta$ monomer, this corresponds to an assembly growth curve, as shown in figure 3B. The NMR experiment enables monitoring fibre growth of $A\beta_{(11-40)}$ and $A\beta_{(1-40)}$ independently from within an equimolar mixture. The lag-times are almost identical for both peptides at 7.5 hours whilst the apparent elongation rates k_{app} are also very similar; 0.15 and 0.17 (± 0.02) hrs^{-1} for $A\beta_{(1-40)}$ and $A\beta_{(11-40)}$ respectively. This strongly suggests that, in the case of $A\beta_{(1-40)}$ and $A\beta_{(11-40)}$, the fibres largely co-fibrillise. It is notable that for similar NMR experiments on $A\beta_{(1-40)}$ with $A\beta_{(1-42)}$ mixtures, which do not co-fibrillise, very different fibre growth curves were obtained for the two isoforms [10b] [10d].

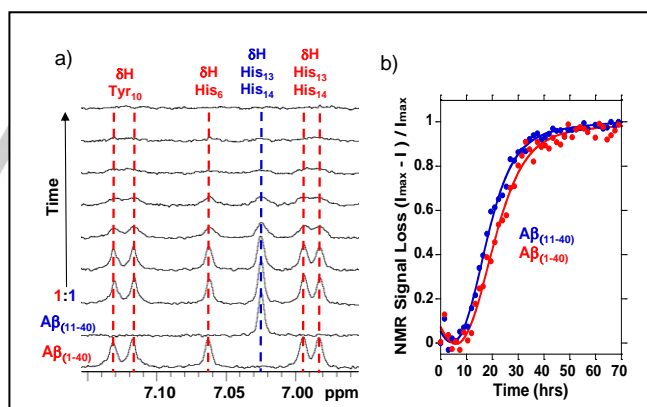


Figure 3: Fibrillation of an equimolar mixture of $A\beta_{(11-40)}$ with $A\beta_{(1-40)}$, 20 μM , monitored by $^1\text{H-NMR}$. Spectra of $A\beta_{(11-40)}$ and $A\beta_{(1-40)}$, along with the 1:1 mixture and subsequent loss of signal over time (a). Time course of the integrated His δH resonances for $A\beta_{(11-40)}$ and $A\beta_{(1-40)}$ peptides at pH 7.4 (b).

Next we investigated the ability for small amounts of fibres from different $A\beta$ isoforms to nucleate fibre formation of the monomeric $A\beta_{(1-40)}$, figure 4. As expected, addition of small amounts of $A\beta_{(1-40)}$ fibre seeds (10%) reduces the lag-times for fibre formation of $A\beta_{(1-40)}$ monomer, figure 4. Similarly $A\beta_{(11-40)}$ fibres were able to cross-seed $A\beta_{(1-40)}$ fibre formation to the same extent, supporting the assertion these two isoforms, with the same C-terminus, are able to co-fibrillise. In contrast, nucleating seeds with the longer C-terminus; $A\beta_{(11-42)}$ and $A\beta_{(1-42)}$ do not accelerate $A\beta_{(1-40)}$ fibre formation. The cross-seeding

experiments show co-fibrillation of $A\beta_{(1-40)}$ with $A\beta_{(11-40)}$ occurs at the elongation and/or secondary surface nucleation stage of assembly. While $A\beta_{(11-42)}$ fibres do not cross-seed $A\beta_{(1-40)}$ fibre formation, see supplemental figure S9 for details.

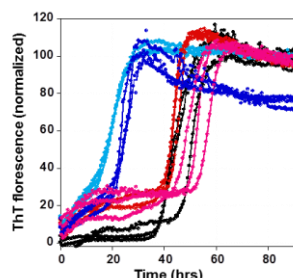


Figure 4: Seeded fibre formation of monomeric $A\beta_{(1-40)}$. In the absence (black) and presence of a 10 % nucleating fibre seed. $A\beta_{(1-40)}$ is nucleated by $A\beta_{(1-40)}$ (pale blue) and $A\beta_{(1-40)}$ (dark blue), but not by $A\beta_{(1-42)}$ (red) or $A\beta_{(11-42)}$ seeds (pink) at pH 7.4, $A\beta_{(1-40)}$ 10 μ M, $n = 3$ traces.

Studies on the assembly of $A\beta_{(1-40)}$ with $A\beta_{(1-42)}$ show that for the C-terminal truncations the two isoforms interact during early oligomerization, but go on to form fibres independently^[10d, 10e]. The lack of co-assembly between $A\beta_{(1-40)}$ with $A\beta_{(1-42)}$ is presumably due to the marked differences in their respective fibre structures, with a U-shaped topology for $A\beta_{(1-40)}$ and S-shaped topology for $A\beta_{(1-42)}$ fibril cores^[12]. This structural difference is centred on the formation of a salt-bridge between Lys28 and the C-terminal carboxylate of Ala42^[12a]. In contrast to the loss of two residues at the C-terminus, our fibre formation kinetics, TEM and ¹H-NMR suggest that the loss of 10 residues from the N-terminus does not prevent fibre co-assembly of $A\beta_{(1-40)}$ with $A\beta_{(11-40)}$. Very different interactions take place for $A\beta_{(11-40)}$ mixed with $A\beta_{(1-42)}$; the formation of fibres for this combination of isoforms is biphasic and is frustrated. These observations suggest that fibre structural topology is unaffected by the loss of the first ten N-terminal residues and so there is little difference in the affinity of $A\beta_{(1-40)}$ or $A\beta_{(11-40)}$ monomer addition to the ends of growing mixed fibres, which facilitates co-fibrillation, see supplemental figure S10.

$A\beta_{(11-40/42)}$ assemblies are a major component (one fifth) of plaques and CSF^[5-6]. The accelerated assembly of $A\beta$ in the presence of N-terminally truncated $A\beta$ has profound ramifications for plaque formation and AD pathology. The impact on mechanical stability of co-assembled fibres also has implications for their neurotoxicity, as fragmented fibres are thought to be more cytotoxic^[14]. There are a number of other $A\beta$ isoforms truncated or extended at both the N- and C-termini^[2, 4]. It may be that truncations at the N-terminus such as $A\beta_{(4-40/42)}$ and $A\beta_{(3-40/42)}$ will also accelerate fibre formation and allow co-fibrillation of their full-length counterparts. Indeed co-fibrillation has been reported for the N-terminal extended isoform of $A\beta$ ^[4a]. In contrast, $A\beta$ truncations at the C-terminus impact fibre structural topology^[12a, 14] and do not co-assemble and consequently cause the frustration of fibre formation kinetics.

Acknowledgements

H. Toms for assistance with NMR experiments. This work was supported by Biotechnology and Biological Sciences Research Council (BBSRC) Code: BB/M023877/1.

Keywords Amyloid beta-peptides • Fibre Kinetics • Co-assembly • Truncation • Protein folding

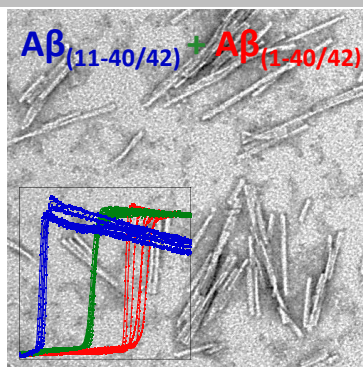
- [1] J. A. Hardy, G. A. Higgins, *Science* **1992**, *256*, 184-185.
- [2] M. P. Kummer, M. T. Heneka, *Alzheimers Res Ther* **2014**, *6*, 28.
- [3] a) R. Vassar, B. D. Bennett, S. Babu-Khan, S. Kahn, E. A. Mendiaz, P. Denis, D. B. Teplow, S. Ross, P. Amarante, R. Loeloff, Y. Luo, S. Fisher, J. Fuller, S. Edenson, J. Lile, M. A. Jarosinski, A. L. Biere, E. Curran, T. Burgess, J. C. Louis, F. Collins, J. Treanor, G. Rogers, M. Citron, *Science* **1999**, *286*, 735-741; b) J. T. Huse, K. N. Liu, D. S. Pijak, D. Carlin, V. M. Y. Lee, R. W. Doms, *Journal of Biological Chemistry* **2002**, *277*, 16278-16284.
- [4] a) O. Szczepankiewicz, B. Linse, G. Meisl, E. Thulin, B. Frohm, C. Sala Frigerio, M. T. Colvin, A. C. Jacavone, R. G. Griffin, T. Knowles, D. M. Walsh, S. Linse, *J Am Chem Soc* **2015**, *137*, 14673-14685; b) M. Wulff, M. Baumann, A. Thummler, J. K. Yadav, L. Heinrich, U. Knupfer, D. Schlenzig, A. Schierhorn, J. U. Rahfeld, U. Horn, J. Balbach, H. U. Demuth, M. Fandrich, *Angew Chem Int Ed Engl* **2016**, *55*, 5081-5084.
- [5] a) P. Seubert, C. Vigo-Pelfrey, F. Esch, M. Lee, H. Dovey, D. Davis, S. Sinha, M. Schlossmacher, J. Whaley, C. Swindlehurst, et al., *Nature* **1992**, *359*, 325-327; b) L. Miravalle, M. Calero, M. Takao, A. E. Roher, B. Ghetti, R. Vidal, *Biochemistry* **2005**, *44*, 10810-10821; c) D. L. Miller, I. A. Papayannopoulos, J. Styles, S. A. Bobin, Y. Y. Lin, K. Biemann, K. Iqbal, *Arch Biochem Biophys* **1993**, *301*, 41-52.
- [6] a) J. Naslund, A. Schierhorn, U. Hellman, L. Lannfelt, A. D. Roses, L. O. Tjernberg, J. Silberring, S. E. Gandy, B. Winblad, P. Greengard, et al., *Proc Natl Acad Sci U S A* **1994**, *91*, 8378-8382; b) K. Liu, I. Solano, D. Mann, C. Lemere, M. Mercken, J. Q. Trojanowski, V. M. Lee, *Acta Neuropathol* **2006**, *112*, 163-174.
- [7] C. P. Sullivan, E. A. Berg, R. Elliott-Bryant, J. B. Fishman, A. C. McKee, P. J. Morin, M. A. Shia, R. E. Fine, *Neurosci Lett* **2011**, *505*, 109-112.
- [8] a) S. Sudoh, Y. Kawamura, S. Sato, R. Wang, T. C. Saido, F. Oyama, Y. Sakaki, H. Komano, K. Yanagisawa, *J Neurochem* **1998**, *71*, 1535-1543; b) C. Russo, G. Schettini, T. C. Saido, C. Hulette, C. Lippa, L. Lannfelt, B. Ghetti, P. Gambetti, M. Tabaton, J. K. Teller, *Nature* **2000**, *405*, 531-532.
- [9] D. Scheuner, C. Eckman, M. Jensen, X. Song, M. Citron, N. Suzuki, T. D. Bird, J. Hardy, M. Hutton, Kukull, W., E. Larson, E. Levy-Lahad, M. Viitanen, E. Peskind, P. Poorkaj, G. Schellenberg, *Nat. Med.* **1996**, *2*, 864-870.
- [10] a) A. Jan, O. Gokce, R. Luthi-Carter, H. A. Lashuel, *J. Biol. Chem.* **2008**, *283*, 28176-28189; b) K. Pauwels, T. L. Williams, K. L. Morris, W. Jonckheere, A. Vandersteen, G. Kelly, J. Schymkowitz, F. Rousseau, A. Pastore, L. C. Serpell, K. Broersen, *J. Biol. Chem.* **2012**, *287*, 5650-5660; c) K. Hasegawa, I. Yamaguchi, S. Omata, F. Gejyo, H. Naiki, *Biochemistry* **1999**, *38*, 15514-15521; d) R. Cukalevski, Yang, X., Meisl, G., Weininger, U., Bernfur, K., Frohm, B., Knowles, T.P.J., Linse, S., *Chemical Science* **2015**, *6*, 4215-4233; e) M. Iljina, G. A. Garcia, A. J. Dear, J. Flint, P. Narayan, T. C. Michaels, C. M. Dobson, D. Frenkel, T. P. Knowles, D. Klenerman, *Scientific reports* **2016**, *6*, 28658.
- [11] J. D. Barritt, J. H. Viles, *J Biol Chem* **2015**, *290*, 27791-27802.
- [12] a) Y. Xiao, B. Ma, D. McElheny, S. Parthasarathy, F. Long, M. Hoshi, R. Nussinov, Y. Ishii, *Nat Struct Mol Biol* **2015**, *22*, 499-505; b) A. K. Paravastu, R. D. Leapman, W. M. Yau, R. Tycko, *Proc Natl Acad Sci U S A* **2008**, *105*, 18349-18354.
- [13] H. A. Scheidt, I. Morgado, S. Rothemund, D. Huster, M. Fandrich, *Angew Chem Int Ed Engl* **2011**, *50*, 2837-2840.
- [14] W. F. Xue, A. L. Hellewell, W. S. Gosal, S. W. Homans, E. W. Hewitt, S. E. Radford, *J Biol Chem* **2009**, *284*, 34272-34282.
- [15] N.D. Younan, J.H. Viles, *Biochemistry* **2015**, *54*, 4297-4306

Entry for the Table of Contents

Layout 1:

COMMUNICATION

Alzheimer's Disease involves the assembly of A β -peptides into toxic oligomers and fibres. A β isoforms of different lengths and aggregation propensities coexist *in vivo* and are able to nucleate or frustrate amyloid co-assembly. We show N-terminally truncated A β accelerates co-assembly and forms rod-shaped fibres with its respective full-length A β counterpart. This has consequences for the toxicity of all A β isoforms.



**Joseph D. Barritt, Nadine D Younan
and John H. Viles***

Page No. – Page No.

N-Terminally Truncated Amyloid- $\beta_{(11-40/42)}$ Co-Fibrillises with its Full-Length Counterpart, Implications for Alzheimer's Disease.